Human Molecular Genetics, 2010, Vol. 19, No. 10 **2039–2049**
doi:10.1093/hmg/ddq085
Advance Access published on February 23, 2010

Pah^{enu1} is a mouse model for tetrahydrobiopterin-responsive phenylalanine hydroxylase deficiency and promotes analysis of the pharmacological chaperone mechanism *in vivo*

Søren W. Gersting[1,†], Florian B. Lagler[3,†], Anna Eichinger[1], Kristina F. Kemter[1], Marta K. Danecka[1], Dunja D. Messing[1], Michael Staudigl[1], Katharina A. Domdey[1], Clemens Zsifkovits[3], Ralph Fingerhut[4,5], Hartmut Glossmann[3], Adelbert A. Roscher[2] and Ania C. Muntau[1,*]

[1]Department of Molecular Pediatrics and [2]Children's Research Center, Dr von Hauner Children's Hospital, Ludwig-Maximilians-University, 80337 Munich, Germany, [3]Department of Medical Genetics, Molecular and Clinical Pharmacology, Innsbruck Medical University, 6020 Innsbruck, Austria, [4]Laboratory Becker, Olgemöller, and colleagues, 81671 Munich, Germany, [5]Newborn Screening Laboratory, University Children's Hospital, 8032 Zurich, Switzerland

Received January 23, 2010; Revised and Accepted February 20, 2010

The recent approval of sapropterin dihydrochloride, the synthetic form of 6[R]-L-*erythro*-5,6,7,8-tetrahydrobiopterin (BH_4), for the treatment of phenylketonuria (PKU) as the first pharmacological chaperone drug initiated a paradigm change in the treatment of monogenetic diseases. Symptomatic treatment is now replaced by a causal pharmacological therapy correcting misfolding of the defective phenylalanine hydroxylase (PAH) in numerous patients. Here, we disclose BH_4 responsiveness in *Pah*^{enu1}, a mouse model for PAH deficiency. Loss of function resulted from loss of PAH, a consequence of misfolding, aggregation, and accelerated degradation of the enzyme. BH_4 attenuated this triad by conformational stabilization augmenting the effective PAH concentration. This led to the rescue of the biochemical phenotype and enzyme function *in vivo*. Combined *in vitro* and *in vivo* analyses revealed a selective pharmaceutical action of BH_4 confined to the pathological metabolic state. Our data provide new molecular-level insights into the mechanisms underlying protein misfolding with loss of function and support a general model of pharmacological chaperone-induced stabilization of protein conformation to correct this intracellular phenotype. *Pah*^{enu1} will be essential for pharmaceutical drug optimization and to design individually tailored therapies.

INTRODUCTION

The biological and medical significance of protein misfolding as a basis of disease is increasingly recognized. Distinct pathophysiological mechanisms underlying protein misfolding disorders are known. In neurodegenerative diseases such as Alzheimer's or Parkinson's disease, misfolded proteins accumulate and form insoluble aggregates associated with molecular and clinical dysfunction (1–3). In other disorders, missense mutations cause unfavorable structural rearrangements resulting in conformational destabilization, rapid degradation and a lack of the functional protein (4–8). The latter group of protein misfolding diseases with loss of function now comes into focus of research. More than 20 monogenetic [e.g. cystic fibrosis, phenylketonuria (PKU)] and acquired (e.g. p53 mutations) disorders are known to be associated with this molecular phenotype (Supplementary Material, Table S1).

*To whom correspondence should be addressed. Tel: +49 8951602746; Fax: +49 8951607952; Email: ania.muntau@med.lmu.de
†The authors wish it to be known that, in their opinion, the first two authors should be regarded as joint First Authors.

Pharmacological chaperones are small-molecule chemical compounds that manipulate dysfunctional biological systems by stabilizing protein conformation in misfolding diseases (7–11). The first pharmacological chaperone drug, BH_4 (Kuvan®), was approved in 2008 for the treatment of PKU (MIM 261600), the most frequent genetic disorder of amino acid catabolism. Pharmacological doses of BH_4, the natural cofactor of the deficient enzyme phenylalanine hydroxylase (PAH), restore enzyme function by a mechanism other than its cofactor action in a significant share of patients (12). First *in vitro* studies using purified PAH pointed to stabilization of the misfolded protein against denaturation and degradation (13–16). In wild-type (17,18) and transgenic mice with deficiency in BH_4 biosynthesis (19), supplementation of BH_4 enhanced the amount of hepatic wild-type PAH protein and *in vivo* enzyme activity. However, an animal model showing the particular phenotype of BH_4-responsive PAH deficiency was not available for approval. This precluded the elucidation of the molecular mechanisms causing loss of function and the mode of action underlying pharmacological chaperone therapy *in vivo*. The aim of this study, therefore, was to identify a mouse model for BH_4-responsive PAH deficiency that would enable *in vitro* and *in vivo* experimental insight into the biological processes associated with PAH deficiency and into the mechanisms of therapeutic correction of the loss-of-function phenotype at the molecular level.

Two mouse strains produced by germline mutagenesis harboring defective *Pah* genes are available (20). The V106A mutation in Pah^{enu1} leads to a mild hyperphenylalaninemia phenotype (21), whereas Pah^{enu2} (F263S) shows severe PKU (www.pahdb.mcgill.ca) (20,22,23). Although Pah^{enu1} was thoroughly studied (20–24), it was not recognized to be a model for the new clinical entity of BH_4-responsive PKU.

The present study disclosed misfolding-induced PAH deficiency and its pharmacological rescue by BH_4 in Pah^{enu1}, reflecting the situation in human hyperphenylalaninemia. Besides accelerated degradation, we observed aggregate formation of the PAH protein *in vitro* and *in vivo*, revealing a novel pathophysiological aspect of protein misfolding in the particular group of conformational disorders with loss of function. Moreover, we showed that BH_4 corrects the biochemical phenotype by stabilizing the target protein conformation, and we retraced the mode of action of the pharmacological chaperone on misfolding, aggregation and degradation of the PAH protein *in vivo*. The animal model presented provided insights into general mechanisms underlying protein misfolding with loss of function and helped to understand the pharmacological chaperone effect of BH_4 at a molecular level. This knowledge will allow us to exploit the resources of chemical compound libraries to design future therapeutic agents for other protein misfolding diseases.

RESULTS

Murine PAH is a suitable model for the human phenylalanine hydroxylating system

It was previously hypothesized that the total activity of murine PAH is higher than that of human PAH due to differences in PAH regulation by substrate and cofactor (22,25). We re-evaluated whether *Mus musculus* is a suitable model for issues related to human PAH by generating the first complete kinetic data from recombinant murine PAH proteins.

Table 1. Steady-state enzyme kinetic parameters of human and murine PAH proteins

Species	Specific activity[a] (nmol Tyr/min × mg protein)	$[S]_{0.5}$[b] (μM)	K_m[c] (μM)	h[b]	Activation fold
WT-HsPAH	3115 ± 149	155 ± 6	24.0 ± 3	3.0	3.0
WT-MmPAH	2628 ± 293	175 ± 34	22.0 ± 5	2.6	3.1

Recombinant tetrameric human (WT-HsPAH) and murine (WT-MmPAH) wild-type PAH were expressed as MBP–PAH fusion proteins in *E. coli*. Apparent affinities for L-phenylalanine ($[S]_{0.5}$), BH_4 (K_m) and the Hill coefficient (h) as a measure of cooperativity are shown. Activation fold represents substrate activation as the ratio of specific activity with and without prior incubation with L-phenylalanine. Values are given as means ± SEM of $n = 3$ experiments.
[a]Specific activity was determined at standard L-phenylalanine (1 mM) and BH_4 (75 μM) concentrations with L-phenylalanine pre-incubation.
[b]Apparent affinities for L-phenylalanine ($[S]_{0.5}$) and the Hill coefficient (h) were determined at variable L-phenylalanine concentrations (0–4.5 mM) and standard BH_4 concentration (75 μM).
[c]Apparent affinities for BH_4 (K_m) were determined at variable BH_4 concentrations (0–700 μM) and standard L-phenylalanine concentration (1 mM).

The specific activity of tetrameric murine wild-type PAH expressed in *E. coli* as fusion protein with maltose binding protein (MBP) was well comparable to that of human wild-type PAH. Apparent affinities of the enzymes for the substrate L-phenylalanine and the BH_4 cofactor, cooperativity for substrate binding and substrate-induced enzyme activation did not differ significantly between murine and human PAH (Table 1). However, total PAH enzyme activity and the PAH protein amount in crude liver lysates of wild-type mice were about twice as high as in human liver (Fig. 1A). Thus, murine and human PAH show similar specific activity and analogous regulation, whereas the inconsistency between specific and total PAH enzyme activity is due to differences in the PAH protein amount *in vivo*.

Loss of function in Pah^{enu1} is associated with reduced amounts of PAH protein

Next, we related specific enzyme activity *in vitro* to residual protein amount and enzyme function *in vivo*. ^{13}C-phenylalanine breath tests assessing phenylalanine oxidation are a good measure for overall *in vivo* PAH activity in humans as well as in mice (12,17,26). The cumulative recovery of $^{13}CO_2$ representing ^{13}C-phenylalanine turnover was 33% for Pah^{enu1} and 12% for Pah^{enu2} when compared with wild-type mice. The mild reduction in enzyme activity in Pah^{enu1} still induced an increase in mean blood phenylalanine concentration to 189 μmol/l (wild-type 76 μmol/l), reflecting a mild hyperphenylalaninemia phenotype, whereas Pah^{enu2} showed phenylalanine concentrations in the range of classical PKU (1144 μmol/l) (Fig. 1B). Data for PAH activity and blood phenylalanine levels are in agreement with previous studies using crude liver lysates (17,22).

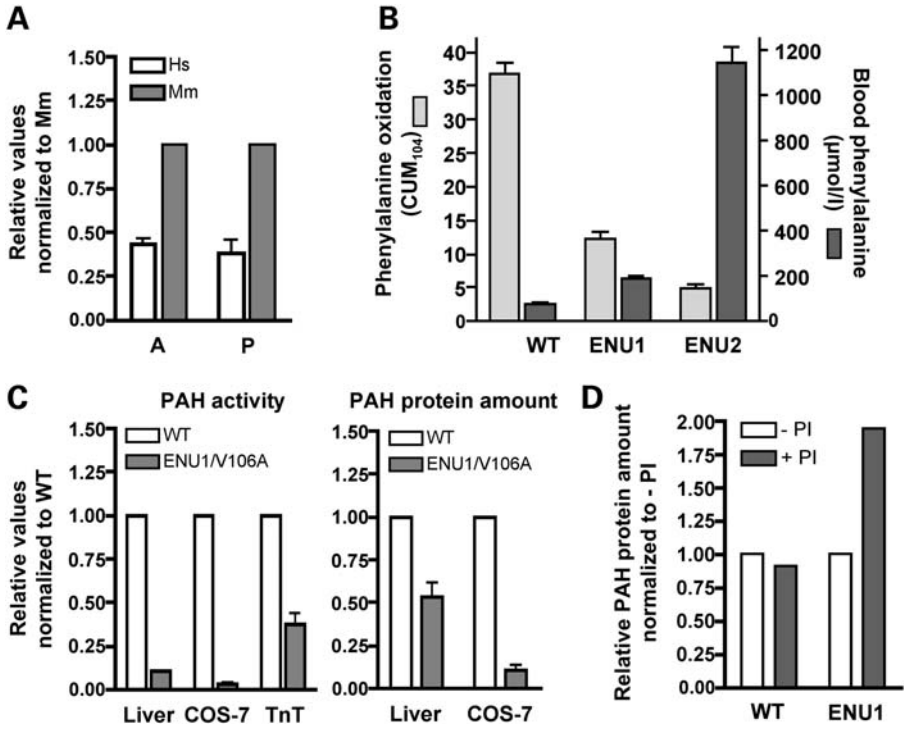

Figure 1. Comparison of human and murine PAH and characterization of PAH deficiency in *Pah*^{enu1} and *Pah*^{enu2} mice. (**A**) Relative PAH activity (A) and PAH protein amount (P) in human and murine crude liver lysates. Data were normalized to murine samples and are given as means ± s.e.m. of $n = 3$ experiments. (**B**) Phenylalanine oxidation and blood phenylalanine levels of wild-type (WT, $n = 6$), *Pah*^{enu1} (ENU1, $n = 10$) and *Pah*^{enu2} (ENU2, $n = 4$) mice *in vivo*. The phenylalanine oxidation rate was assessed by determination of the cumulative $^{13}CO_2$ recovery at 104 min (CUM_{104}) after i.p. application of ^{13}C-phenylalanine (15 µg/g body weight). Values are given as means ± s.e.m. (**C**) Relative PAH activity (left) and PAH protein amount (right) of murine wild-type PAH (WT) and ENU1/V106A-PAH in crude liver lysates, expressed in COS-7 cells and in the TnT system. Data were normalized to WT-PAH and are given as means ± s.e.m of $n = 3$ experiments. (**D**) Protection of PAH protein by protease inhibitors (PI). Liver lysates of wild-type mice (WT) and *Pah*^{enu1} (ENU1) mice in the absence or presence of PI. Data of $n = 1$ experiment were normalized to conditions without PI.

Recombinant expression and purification of variant murine PAH allowed for detailed analysis of the catalytic function of *Pah*^{enu1} (V106A) and *Pah*^{enu2} (F263S). The latter harbors a mutation in the catalytic core, leading to a near-complete loss of specific PAH activity, whereas V106A undergoes loss of function by distinct molecular mechanisms. Compellingly, the V106A replacement in the regulatory domain resulted in unimpaired specific enzyme activity. Likewise, positive cooperativity (h, 2.6) and apparent affinity to the cofactor (K_m, 22.0 µM) were almost identical to wild-type. But still, regulatory characteristics of PAH kinetics were altered with respect to a moderate increase in affinity to the substrate and a complete loss of substrate activation (Table 2). These findings point to a structural change of the V106A variant, which may have adopted a pre-activated 'r-state'-like conformation. Decreased *in vivo* enzyme activity (^{13}C-phenylalanine oxidation) was confirmed by *ex vivo* analyses (liver lysates) and in eukaryotic expression systems (COS-7 cells and TnT) (Fig. 1C). This was attended by a reduced amount of PAH protein in both the physiological context of the liver and the artificial expression system COS-7. These results suggested misfolding-induced proneness of V106A to degradation, potentially mediated by increased proteolytic turnover. Indeed, the presence of protease inhibitors led to an increase in the PAH protein amount in *Pah*^{enu1}, but not in wild-type liver lysates (Fig. 1D).

Table 2. Steady-state enzyme kinetic parameters of wild-type and variant murine PAH proteins

Genotype	Specific activity[a] (% of wild-type)	$[S]_{0.5}$[b] (µM)	K_m[c] (µM)	h[b]	Activation fold
WT	100	175 ± 34	22.0 ± 5	2.6	3.1
V106A	108 ± 14	103 ± 24	22.0 ± 6	2.6	1.0
F263S	4 ± 17	—	—	—	0.8

Recombinant tetrameric wild-type (WT) and variant (V106A, F263S) murine PAH proteins were expressed as MBP–PAH fusion proteins in *E. coli*. Apparent affinities for L-phenylalanine ($[S]_{0.5}$), BH_4 (K_m) and the Hill coefficient (h) as a measure of cooperativity are shown. Activation fold represents the ratio of specific activity with and without prior incubation with L-phenylalanine. Values are given as means ± s.e.m. of $n = 3$ experiments. The marked reduction in the specific PAH activity of F263S precluded the determination of further enzyme kinetic parameters.

[a]Specific activity was determined at standard L-phenylalanine (1 mM) and BH_4 (75 µM) concentrations with L-phenylalanine pre-incubation.

[b]Apparent affinities for L-phenylalanine ($[S]_{0.5}$) and the Hill coefficient (h) were determined at variable L-phenylalanine concentrations (0–4.5 mM) and standard BH_4 concentration (75 µM).

[c]Apparent affinities for BH_4 (K_m) were determined at variable BH_4 concentrations (0–700 µM) and standard L-phenylalanine concentration (1 mM).

Thus, loss of function in *Pah*^{enu1} is associated with reduced amounts of PAH protein and points to protein misfolding as the pathogenic trigger.

Misfolding induces PAH aggregation and degradation *in vitro*

The protein misfolding phenotype of *Pah*^{enu1} was analyzed by steady state, kinetic and thermal aggregation and degradation assays using recombinant protein. We monitored the oligomeric state of murine wild-type and V106A-PAH following affinity chromatography. Size-exclusion chromatography (SEC) revealed a similar tetramer-to-dimer ratio of both proteins, and this corresponded to human (4,27) and rat PAH (28), although V106A additionally showed a distinct peak of aggregates (Fig. 2A). Blue native polyacrylamide gel electrophoresis (BN-PAGE) showed tetramers, dimers and monomers in an apparent equilibrium for wild-type and variant PAH, with V106A displaying more high-molecular-weight aggregates and a higher amount of degradation fragments than the wild-type (Fig. 2B). Subsequent analyses focussed on the active enzyme homo-oligomer obtained by the separation of the tetrameric SEC fraction. The determination of particle sizes by dynamic light scattering (DLS) at the steady state revealed two populations for the wild-type corresponding to native-state protein and soluble aggregates in equilibrium. For V106A, a shift towards the non-native state was observed (Fig. 2C). Analysis of kinetics of soluble aggregate formation over time resulted in a significantly ($P = 0.0037$) higher exponential growth rate constant for V106A ($k = 0.072$) than for the wild-type ($k = 0.041$) (Fig. 2D).

Differential scanning fluorimetry (DSF) showed increased ground state hydrophobicity of V106A in comparison to the wild-type, indicating the presentation of non-native state hydrophobic groups at the protein surface. Thermal unfolding disclosed a two-phase transition from native to the unfolded state for wild-type and V106A. This corresponds to human PAH, where the first transition reflects unfolding of the regulatory and the second unfolding of the catalytic domain (4,29) (Fig. 2E). Although the shape and total height of the curves differed, midpoints of the first and second transitions were similar for wild-type and V106A.

The impact of local unfolding on protein stability as well as the equilibrium between native-state oligomeric protein and potential folding intermediates was further analyzed by limited proteolysis (30,31). Compared with the wild-type, V106A revealed degradation bands even without the addition of proteinase K and showed a different fragmentation pattern (Fig. 2F). The half-life of the intact PAH band (52 kDa) after the proteolytic cleavage of the MBP fusion partner was prolonged for V106A (34 min) in comparison to the wild-type (13 min). This finding may be explained by the fact that aggregates not attacked by proteinase K could appear as intact PAH in a denaturating SDS–PAGE.

Taken together, the equilibrium of native-state and partially unfolded or misfolded protein is shifted towards a distorted V106A conformation, explaining proneness to aggregation and susceptibility to degradation.

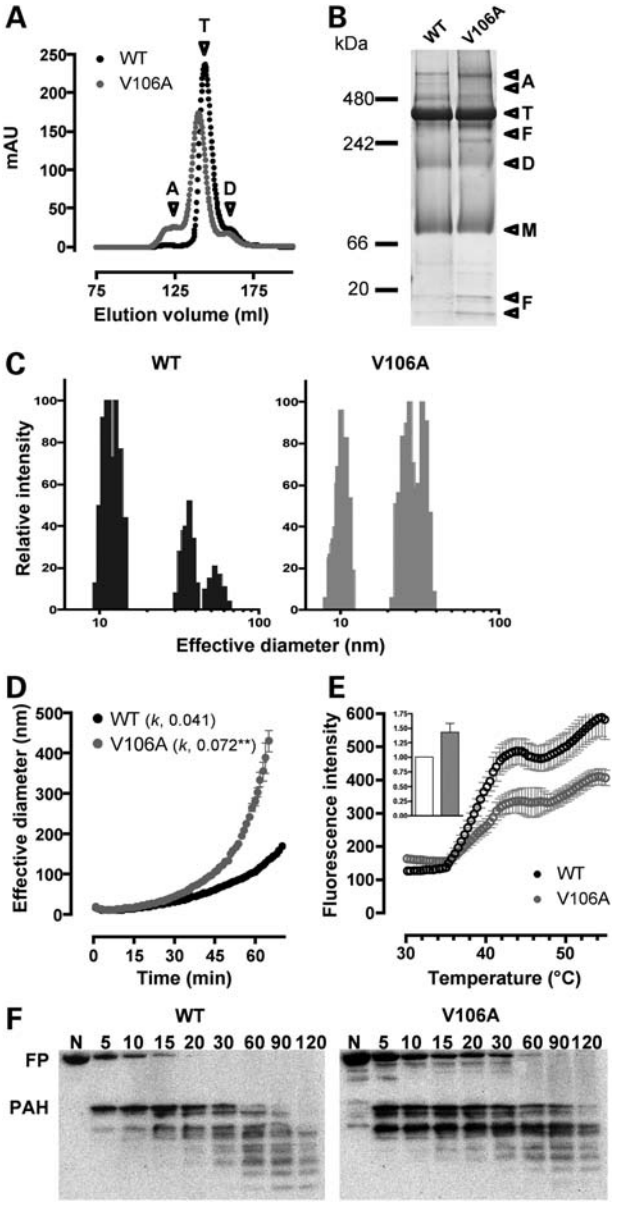

Figure 2. Impact of the V106A mutation on PAH protein conformation *in vitro*. Wild-type (WT) and V106A-PAH were expressed as fusion protein to MBP, purified by affinity chromatography and tetrameric MBP–PAH was separated by SEC. (**A**) Oligomerization profiles (normalized to tetrameric WT) determined by SEC. Arrows indicate soluble aggregates (A, 120 ml), tetramers (T, 140 ml) and dimers (D, 158 ml). (**B**) BN-PAGE analysis of affinity-purified protein. Arrows indicate aggregates (A), tetramers (T, 380 kDa), dimers (D, 190 kDa), monomers (M, 95 kDa) and degradation fragments (F). (**C**) Particle size distribution of the tetrameric SEC fraction determined by DLS. The cumulative relative occurrences (relative intensity, *y*-axis) of particles with distinct effective diameters (*x*-axis) of $n = 3$ independent experiments are shown. Expected diameter for tetrameric MBP–PAH is 16 nm. (**D**) Aggregation kinetics measured by DLS. The rate constants (k) of changes in the effective diameter of the protein are given and the significance is indicated ($^{**}P < 0.01$). Data points represent means ± s.e.m. of $n = 3$ experiments. (**E**) Thermal denaturation analyzed by DSF. Data points represent means ± s.e.m. of $n = 3$ experiments. The inset shows the fluorescence at 30°C normalized to WT. (**F**) Proteolytic degradation patterns of MBP–PAH fusion proteins. Samples were incubated without proteinase K (N) or for 5–120 min at 37°C with proteinase K. Fusion proteins (FP), the cleaved-off PAH protein (PAH) and proteolytic fragments of PAH were detected. One representative experiment out of four is shown for WT and V106A.

BH_4 rescues loss of function *in vivo*

We showed that *Pah*^{enu1} has the same pathophysiological background of protein misfolding with loss of function as that associated with human *PAH* mutations (4,14,16). We

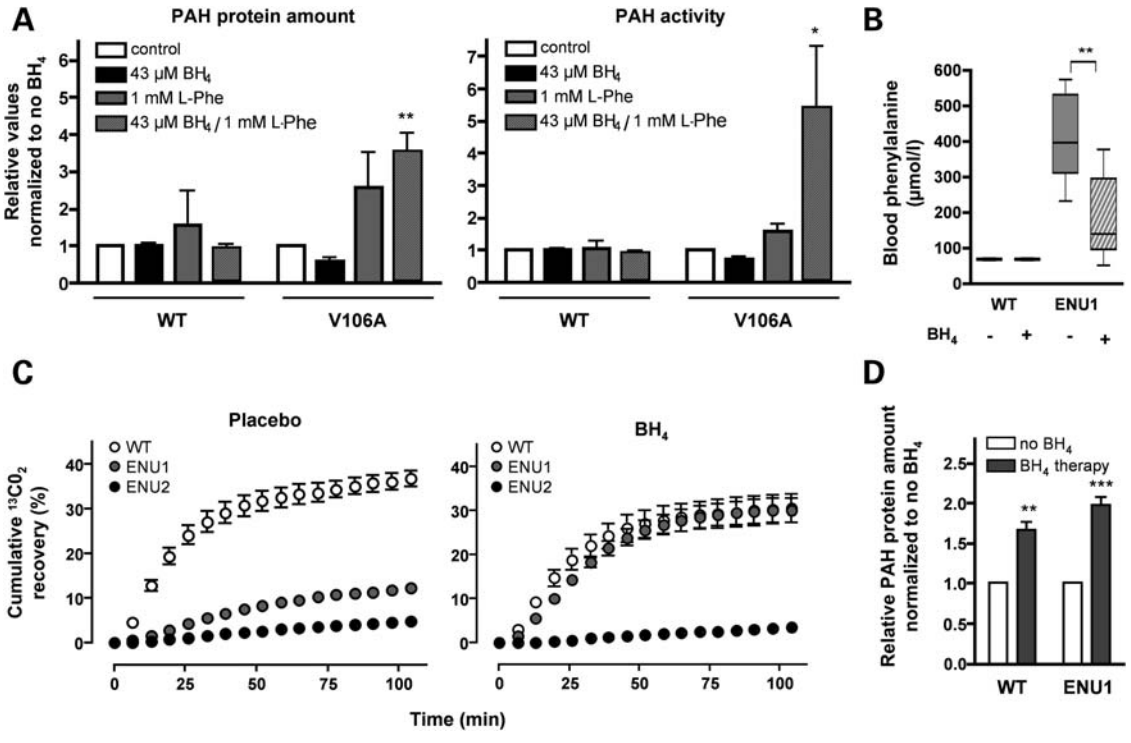

Figure 3. BH_4 stabilizes the PAH protein and corrects loss of function *in vivo*. (**A**) Wild-type (WT) and V106A-PAH proteins were overexpressed in COS-7 cells for 72 h and cultured in basic medium (RPMI 1640, L-phenylalanine 96 μM; control). The medium was supplemented with either BH_4 (43 μM), additional L-phenylalanine (final concentration 1 mM) or both BH_4 and L-phenylalanine as indicated. Data were normalized to the control and significances relative to the control are indicated ($^*P < 0.05$, $^{**}P < 0.01$). Bars represent means ± s.e.m. of $n = 5$ experiments. (**B**) Basic blood phenylalanine levels before and after BH_4 therapy. Wild-type (WT) and *Pah*^{enu1} (ENU1) mice were treated with either 20 μg BH_4/g bw or placebo for 3 days in two single doses per day. Box plots represent blood phenylalanine levels of $n = 4$ (WT) and $n = 7$ (ENU1) animals and the significance is indicated ($^{**}P < 0.01$). (**C**) Phenylalanine oxidation rates determined by a ^{13}C-phenylalanine breath test. Mice were treated with BH_4 (20 μg/g bw) or placebo and the cumulative CO_2 recovery was monitored in $n = 6$ animals for each genotype and is given as mean values ± s.e.m. (**D**) Relative amounts of PAH protein in liver lysates after treatment with BH_4 (20 μg/g bw for 3 days). Data were normalized to mice that received placebo and are given as means ± s.e.m. of $n = 3$ experiments. $^{**}P < 0.01$, $^{***}P < 0.001$.

now aimed to analyze whether the pharmacological chaperone BH_4 corrects these alterations. In our wild-type mice, one single dose of 10 μg/g body weight (bw), commonly used in the treatment of PAH-deficient patients, led to a liver peak concentration of 43 μmol/l BH_4 30 min after injection. Hence, this concentration was used for the following experiments in cell culture and *in vitro*.

The effect of BH_4 on PAH protein amount and enzyme activity was first characterized after transient expression of wild-type and V106A-PAH in COS-7 cells (Fig. 3A). Treatment with BH_4 at low phenylalanine concentrations (96 μmol/l in the medium) did not result in a rise of protein amount or enzyme activity in wild-type or V106A. Notably, pathologically high phenylalanine concentrations (1 mM) produced a mild increase in the amount of wild-type and, more pronounced, of the V106A-PAH protein. However, this had no perceptible effect on enzyme activity. Only the application of BH_4 at high phenylalanine concentrations resulted in a significant increase in V106A-PAH protein amount ($P < 0.01$) and activity ($P < 0.05$), suggesting that the pharmacological chaperone exerts its action predominantly at harmful substrate levels.

BH_4 treatment *in vivo* (2 × 10 μg/g bw × d, 3 days) significantly ($P < 0.01$) lowered blood phenylalanine concentrations (median, 396–139 μmol/l) in *Pah*^{enu1}, while the wild-type remained at physiological levels (median, 68 μmol/l) (Fig. 3B). The therapeutic effect of BH_4 on hyperphenylalaninemia was functionally confirmed by placebo-controlled ^{13}C-phenylalanine oxidation tests, demonstrating rescue of *in vivo* PAH activity. Treatment normalized $^{13}CO_2$ recovery in *Pah*^{enu1} to wild-type levels, whereas it had no effect in *Pah*^{enu2} (Fig. 3C). This was attended by a significant increase in liver PAH protein in the wild-type ($P < 0.01$) and, even more pronounced, in *Pah*^{enu1} ($P < 0.001$) (Fig. 3D).

These data show that BH_4 corrects the biochemical phenotype of *Pah*^{enu1} through stabilization of the PAH protein *in vivo*. Moreover, the pharmacological chaperone-mediated rescue of enzyme function requires an imbalanced metabolic state reflected by hyperphenylalaninemia and sufficient specific residual enzyme activity.

BH_4 corrects protein misfolding

To dissect the molecular mode of action of the pharmacological chaperone BH_4 at the protein level, we analyzed its effect on PAH misfolding/unfolding, aggregation and degradation. The addition of BH_4 (43 μM) significantly ($P < 0.01$) reduced the increased hydrophobicity of recombinant V106A, while it had no effect on the wild-type protein (Fig. 4A). Native-state stabilization with respect to the

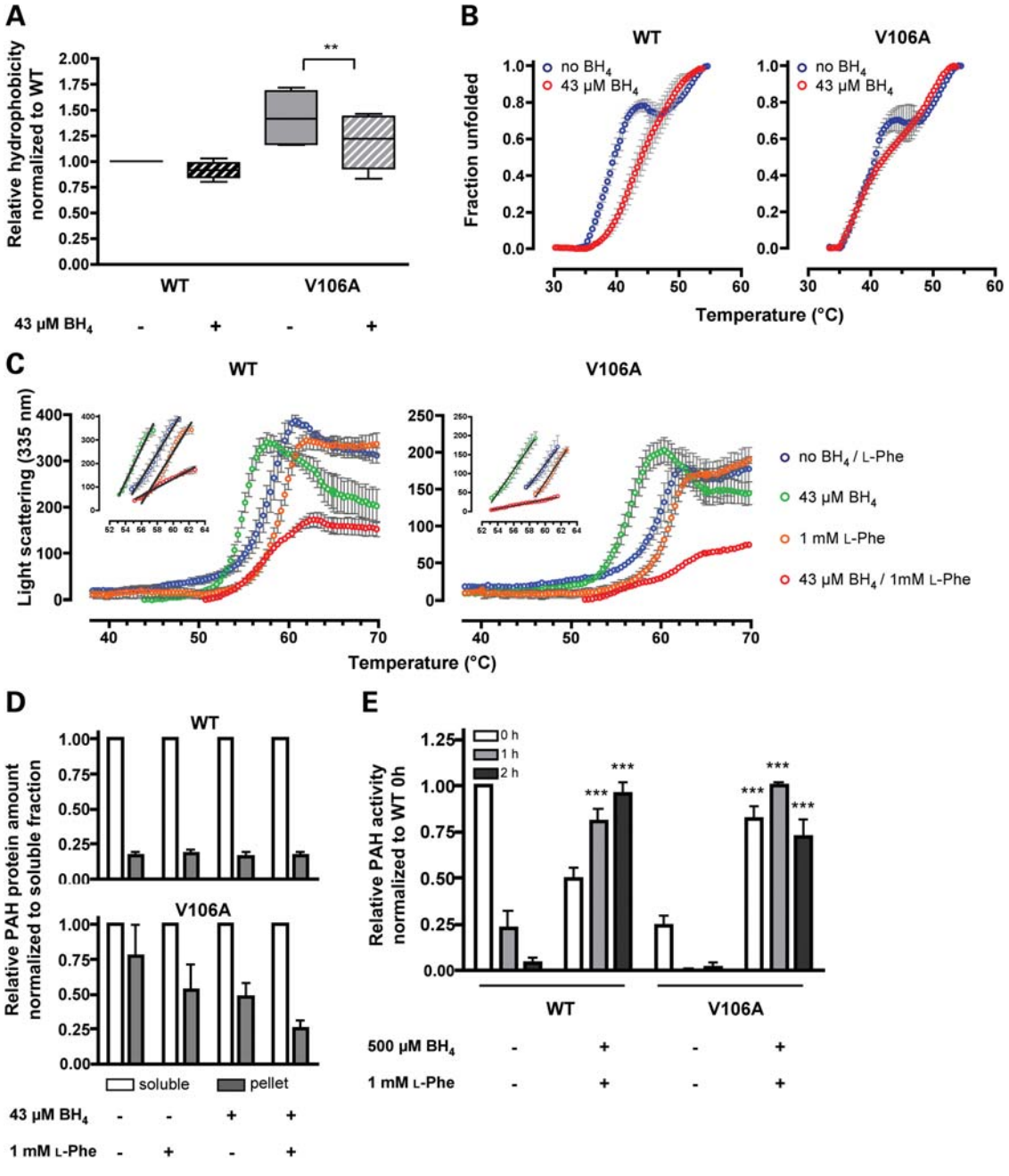

Figure 4. BH_4 prevents PAH aggregation and degradation. (**A**) Relative hydrophobicity of wild-type (WT) and V106A-PAH proteins determined by ANS fluorescence at 25°C with and without the addition of BH_4 (43 μM). Plots represent ANS-fluorescence values normalized to WT without BH_4 of $n = 4$ experiments and the significance is indicated (**$P < 0.01$). (**B**) Thermal unfolding of wild-type (WT) and V106A-PAH with and without the addition of BH_4 (43 μM) monitored by ANS fluorescence. The fractions of unfolded PAH protein are plotted as a function of increasing temperatures. Data points represent the mean ± s.e.m. of $n = 3$ experiments. (**C**) Temperature-induced aggregation of wild-type (WT) and V106A-PAH observed by RALS. Aggregate formation in the presence or absence of BH_4 (43 μM) and L-phenylalanine (1 mM) was detected. For the linear phase of aggregation, the transition midpoints and the slopes of the curves were calculated by linear regression analysis (Table 3). The insets depict the slopes at the linear phase of aggregation. Data points and calculated values represent means ± s.e.m. of $n = 3$ experiments. (**D**) Aggregation of WT and V106-PAH protein expressed in COS-7 cells upon treatment with BH_4 (43 μM) and/or L-phenylalanine (1 mM). The PAH amount in the soluble and pellet fractions was detected. Bars are normalized to the soluble fraction and represent means ± s.e.m. of $n = 4$ experiments. (**E**) Protection against degradation-induced loss of PAH function in a eukaryotic TnT system. Wild-type (WT) and V106A-PAH were expressed with or without the addition of BH_4 (500 μM) and L-phenylalanine (1 mM) as indicated. The reaction was stopped and the relative activity was assessed following further incubation for 0, 1 or 2 h at 37°C. Significances of changes in relation to the control (no BH_4/L-phenylalanine) are indicated (***$P < 0.001$). Data are normalized to wild-type activity at time point 0 and bars represent means ± s.e.m. of $n = 3$ experiments.

midpoint of unfolding (T_m) was observed upon application of thermal stress (wild-type, 38.96–44.15°C, $P = 0.042$; V106A, 40.39–42.01°C, $P = 0.184$). BH_4 induced a right shift of the low-temperature transition, indicating stabilization of the regulatory domain of the proteins, which was more pronounced in the wild-type (Fig. 4B). The minor effect for

Table 3. Parameters of aggregation kinetics assessed by RALS

	WT $T_{m1/2}$ (°C)	Slope	V106A $T_{m1/2}$ (°C)	Slope
No BH_4/L-Phe	57.20 ± 0.07	55.31 ± 3.46	58.95 ± 0.09	27.24 ± 4.07
43 μM BH_4	54.54 ± 0.03	69.44 ± 3.92	55.85 ± 0.06	30.19 ± 1.95
1 mM L-Phe	58.76 ± 0.05	54.54 ± 2.22	60.29 ± 0.06	31.64 ± 1.99
43 μM BH_4 / 1 mM L-Phe	57.14 ± 0.06	18.09 ± 0.68	59.09 ± 0.10	4.00 ± 0.17

Temperature induced aggregation of wild-type (WT) and V106A-PAH observed by RALS. Aggregate formation in the presence or absence of 43 μM BH4 and 1 mM L-phenylalanine was detected. Transition midpoints ($T_{m1/2}$) defined as the temperature at half-maximum aggregation were calculated by nonlinear regression analysis using the Boltzman sigmoidal equation. For the linear phase of aggregation, the slopes of the curves were calculated by linear regression analysis. Values represent means ± s.e.m. of $n = 3$ experiments.

V106A may be attributed to a conformational rearrangement of the regulatory domain due to the variant enzyme's pre-activation (Table 2).

Protein aggregate formation upon thermal stress was assessed by right angle light scattering (RALS). Without additives, aggregation occurred in the range between 50 and 60°C and reached a plateau at 60°C (Fig. 4C). Addition of the cofactor BH_4 led to aggregation at lower temperatures, whereas pathological concentrations of the substrate L-phenylalanine (1 mM) led to aggregation at higher temperatures for wild-type and V106A (Table 3). Neither phenylalanine nor BH_4, however, markedly changed the slope of the curves when applied alone. Only the combined application of BH_4 and phenylalanine substantially reduced aggregation rates, with a more pronounced effect in V106A (slope reduced to 14.7% of initial) than in the wild-type (32.7% of initial).

These results were substantiated at the cellular level. In transiently transfected COS-7 cells, wild-type PAH was predominantly found in the soluble fraction with <20% of the protein in the pellet (Fig. 4D). V106A, though, accumulated in the pellet fraction, indicating enhanced aggregation *in vivo*. Supplementation of the medium with BH_4 or phenylalanine (1 mM) moderately reduced variant PAH in the pellet. However, a combined application of BH_4 and phenylalanine markedly decreased aggregation. We then investigated the impact of the pharmacological chaperone BH_4 on PAH activity over time in a eukaryotic TnT system (Fig. 4E). In the absence of BH_4 and phenylalanine, wild-type and V106A activity declined within 1 h, where the initial activity of V106A was lower than that of the wild-type and decreased more rapidly. In the presence of BH_4 and phenylalanine, loss of wild-type and V106A activity was reverted and V106A reached wild-type levels. The initial reduction of wild-type activity upon addition of BH_4 is in line with the inhibitory effect of BH_4 observed in the phenylalanine oxidation tests (Fig. 3C) and reflects the well-known cofactor inhibition of PAH activity (32–34).

In conclusion, BH_4 exerts its effect as a pharmacological chaperone in the *Pah*^{enu1} mouse by stabilization of PAH conformation and thus preventing aggregation and protecting the mutant enzyme from rapid degradation.

DISCUSSION

The relevance of protein misfolding for inherited diseases is increasingly appreciated and novel therapeutic strategies emerge. A substantial number of small-molecule chemical compounds, which either stabilize the distorted protein conformation or restore the function of affected biological pathways, were lately identified (Supplementary Material, Table S1) (7,9–11). One of these is BH_4, recently approved by the FDA and the EMEA as an orphan drug to correct protein misfolding in PAH deficiency. This makes BH_4 the first representative of a new class of pharmaceutical drugs, and further stabilizing compounds for other diseases are likely to follow.

Here, we report that the *Pah*^{enu1} mouse shows BH_4-responsive PAH deficiency and therefore is a model for a treatable protein misfolding disease with loss of function. Although *Pah*^{enu1} displays a biochemical phenotype, the specific PAH activity is normal. We identified loss of PAH protein as a cause of loss of function in this animal model. It is a consequence of misfolding and accelerated degradation of the enzyme. Notably, our *in vitro* and *in vivo* data revealed that aggregation also significantly contributes to loss of function. The elucidation of this triad created the basis to dissect the molecular mode of action of the pharmacological chaperone BH_4 bridging *in vitro* data on protein stabilization to *in vivo* metabolic state and enzyme activity.

The PAH protein is a flexible, highly regulated tetrameric enzyme undergoing conformational changes upon binding of the L-phenylalanine substrate and the natural cofactor BH_4 (35–37). The latter functions as a negative effector to form a dead-end PAH–BH_4 complex *in vivo*. This keeps the enzyme in an inactivated form that is activated by high blood phenylalanine concentrations (38). As previously described for human mutations (4,16), the genetic alteration in this mouse does not lead to changes in PAH affinity to the cofactor or to a marked reduction of specific enzyme activity. Thus, the mode of action of BH_4 in PAH deficiency is not related to its cofactor action. Instead, pharmacological doses of BH_4 lead to protein stabilization augmenting the effective PAH concentration, that is, the amount of correctly folded and functional PAH. This is achieved by decelerating aggregation, reducing protein hydrophobicity and slowing-down degradation. At a structural-mechanistic level, the improved biochemical phenotype is the result of a trade-off between a gain in protein rigidity and a loss of enzyme activity. Whereas wild-type mice display a drug-induced decrease in PAH activity, in *Pah*^{enu1} the increase in effective enzyme concentration overrules the inhibition by BH_4 and thus explains complete correction of enzyme activity *in vivo*. Hence, the chemical compound has a direct influence on PAH protein chemistry, shifting the activated, instable and aggregation-prone conformation towards a less active but stabilized state.

We observed that BH_4 was very effective at high phenylalanine concentrations, whereas it did not increase enzyme activity at low substrate levels. This phenomenon of selective pharmaceutical action adjusted to metabolic needs can be ascribed to the complex regulation of the phenylalanine hydroxylating system known from human and rat PAH (32–34,39), and here confirmed to be analogous in the mouse. The physio-

logical inhibitory action of the cofactor BH_4 is reflected in the pharmacological inoperativeness of the drug at low substrate concentrations. This is of particular importance since it prevents undue elimination of the essential amino acid phenylalanine and thus protects the patient from overtreatment. This makes BH_4 a pharmacological chaperone drug with the ideal characteristic of an integrated self-limiting mechanism considerably improving its safety profile.

The animal model described here will allow for studies leading to significant advances for patients with PKU. It will enable further pharmacological studies that address detailed pharmacodynamics and pharmacokinetics of BH_4 in a mouse displaying the disease-specific phenotype, and it will provide valuable information towards individually tailored treatment strategies by its use to explore BH_4 dosing at various metabolic states. Moreover, an *in vivo* model will be mandatory for the development of optimized BH_4 derivatives and future generations of PAH stabilizing compounds (40) with improved bioavailability and efficacy.

However, the use of *Pah*^{enu1} will not be confined to issues related to PAH. Direct analyses of the misfolded protein's function (*in vivo* enzyme activity) and the biochemical phenotype (metabolite concentrations) in the living animal offer the opportunity to investigate universal cellular pathways modulating loss-of-function pathology. These will include the concerted action of molecular chaperones, the unfolded protein response pathway, and the protein degradation machinery. Moreover, the impact of epigenetic and environmental stress factors, such as single nucleotide polymorphisms, oxidative stress, or fever, which trigger or exacerbate conformational diseases, can be analyzed. Finally, the model may be used to explore the efficacy of alternative compounds or combinatorial therapeutic strategies, where pharmacological chaperones act in synergy with antioxidative substances, proteasome inhibitors or regulators of protein homeostasis (7,11).

In conclusion, our data support a general model of pharmacological chaperone-induced stabilization of protein conformation to correct protein misfolding with loss of function. The knowledge gained and the experimental strategies applied will be applicable to other maladies belonging to this group of disorders and may thus promote the development of new drugs for the treatment of misfolding-associated genetic and non-genetic diseases.

MATERIALS AND METHODS

Plasmid constructs and site-directed mutagenesis

The cDNA of murine *Pah* (EST clone from imaGenes) was cloned into the pcDNA3.1/myc-His C vector (Invitrogen). The mutations V106A and F263S were introduced into the pcDNA3.1 plasmid using the PCR-based QuikChange site-directed mutagenesis kit (Stratagene) and authenticity was verified by DNA sequencing. Subsequently, wild-type and mutant cDNAs were subcloned into the prokaryotic expression vector pMAL-c2E (New England Biolabs) or the eukaryotic expression vector pEF-DEST51 (Invitrogen). In order to create constructs for eukaryotic expression of wild-type and variant PAH, the Gateway technology (Invitrogen) was used. Genes were amplified using primers containing flanking *att*B sites, Kozak sequence at the 5′ terminus (Mm*Pah* forward) and a stop codon at the 3′ terminus (Mm*Pah* reverse) (Supplementary Material, Table S2). Obtained PCR products were subsequently cloned into the pEF-DEST51 vector carrying the human elongation factor promotor (Invitrogen), following the manufacturer's protocols.

Protein expression and purification

Expression plasmids were transformed into *E. coli* DH5α. Wild-type and variant fusion proteins (MBP–PAH) were overexpressed for 20 h at 37°C as described previously (4). Proteins were purified on ÄKTAxpress (GE Healthcare) at 4°C by loading crude extracts on a MBPTrap affinity chromatography column (GE Healthcare) equilibrated with column buffer (20 mM Tris–HCl, 200 mM NaCl, pH 7.4) and by elution with the same buffer supplemented with 10 mM maltose.

PAH activity assay

PAH activity was determined as described previously (27,41) with various modifications (4). Recombinant tetrameric PAH (0.01 mg/ml) was pre-incubated with L-Phe and catalase (1 mg/ml) for 5 min (25°C) in 15 mM Na HEPES, pH 7.3, followed by 1 min incubation with 10 μM ferrous ammonium sulfate. The reaction was initiated by the addition of 6[R]-L-erythro-5,6,7,8-tetrahydrobiopterin (BH_4, Schircks Laboratories) stabilized in 2 mM DTT, carried out for 1 min and stopped by acetic acid, followed by 10 min incubation at 95°C. Kinetic parameters were determined at standard L-Phe (1 mM) and BH_4 (75 μM) concentrations at variable BH_4 (0–704.1 μM) or L-Phe (0–4.5 mM) concentrations, respectively. To determine the level of substrate activation, pre-incubation with the substrate was omitted and the reaction was triggered by simultaneous addition of 1 mM L-Phe and 75 μM BH_4 (activation fold). All concentrations mentioned refer to the final concentration in a 100 μl reaction mixture. The amount of the product (L-tyrosine) was measured by HPLC and assayed as triplicates. In the case of PAH obtained from either cell culture or the TnT system, 20 μl of total lysates were used for the activity assay. The reaction initiated by the addition of BH_4 was carried out for 60 min (cell culture and TnT) or 20 min (liver lysates), respectively. Steady-state kinetic parameters of three independent experiments were calculated by nonlinear regression analysis with the use of GraphPad Prism 4.0c (GraphPad Software). Enzyme kinetic parameters at variable substrate concentrations displayed cooperativity and were calculated with the Hill equation. Enzyme kinetic parameters at variable cofactor concentrations were calculated with the Michaelis–Menten equation. All experimental data were confirmed by repeated analyses of different protein purifications.

Analysis of oligomerization

Oligomerization profiles were obtained by SEC on a HiLoad 26/60 Superdex 200 column (GE Healthcare) equilibrated with SEC buffer (20 mM Na HEPES, 200 mM NaCl, pH 7.0) and relative amounts of the different oligomeric states were

calculated as described previously (4). Protein concentrations were determined spectrophotometrically with the use of the absorption coefficient A_{280} or the Bradford assay. All following experiments using recombinant protein, except for the BN-PAGE analysis, were performed with tetrameric fusion proteins.

Blue native polyacrylamide gel electrophoresis

BN-PAGE was used to analyze non-dissociated protein complexes with respect to composition, oligomeric state and molecular mass. For this purpose, the protein pool of affinity-purified wild-type mouse PAH was separated via native PAGE using 4–16% (w/v) pre-cast polyacrylamide-gradient native gels in a Bis–Tris buffer system (Invitrogen). The electrophoresis was started at 150 V for 60 min and continued for 90 min at 250 V at 4°C. Following BN-PAGE, proteins were denatured in the gel, stained with Coomassie Brilliant Blue R-250 (Bio-Rad) and the oligomeric state was determined in comparison to protein standards (GE Healthcare).

SDS–PAGE and immunoblotting

The proteins were separated by 4–12% gradient polyacrylamide gels (Invitrogen) and blotted onto a nitrocellulose membrane (Schleicher & Schuell BA-S 85). The membrane was blocked with 5% milk in 1× TBS followed by 1 h of incubation with the primary antibody, mouse monoclonal anti-PAH PH8 (Calbiochem, 1 : 1000 dilution), and 1 h of incubation with the secondary antibody, anti-mouse IgG conjugated with alkaline phosphatase (Promega, 1 : 7500 dilution). Blots were visualized with CDP-Star substrate (Roche) and chemiluminescence was monitored with a DIANA III imaging system, and the resulting protein bands were quantified by AIDA software (Raytest).

Dynamic light scattering

DLS analysis was performed on a ZetaPALS particle size analyzer (Brookhaven Instruments Corporation) equipped with a precision Peltier temperature control unit. The steady-state determination of particle sizes of the tetrameric fusion proteins MBP–PAH (10 μM PAH subunit) diluted in SEC buffer was performed at 25 °C at time intervals of 1 min over a period of 10 min in six independent measurements. The kinetics of thermal aggregation over time was monitored at 52°C at time intervals of 1 min until the precipitation of insoluble aggregates. Analysis of three independent experiments was performed by fitting the obtained data to a single exponential growth curve. The scattering angle was 90°.

Limited proteolysis by proteinase K

Experiments were performed as described previously (4). Wild-type and V106A murine MBP–PAH were digested with proteinase K (substrate to protease ratio 1 : 5000) at 37°C in SEC buffer. SDS–PAGE electrophoresis and immunoblotting with anti-PAH antibody were performed and the resulting PAH bands were quantified by AIDA software (Raytest).

Thermal denaturation assays

RALS and DSF analyses were performed on a Cary Eclipse fluorescence spectrophotometer equipped with a temperature-controlled Peltier multicell holder (Varian). Denaturation of protein samples diluted in SEC buffer containing 1 mM DTT was performed by scanning a temperature range of 25–85°C at a rate of 1.2°C/min (25–35°C and 75–85°C) or 0.2°C/min (35–75°C). In the cases indicated, L-phenylalanine (Sigma) and BH_4 were added to final concentrations of 1 mM and 43 μM, respectively. In DSF experiments, the changes in 8-anilino-1-naphtalenesulfonic acid (ANS, Sigma Aldrich) fluorescence emission at 500 nm (excitation 395 nm, slit widths 5.0/10.0 nm) were monitored. Data analysis was performed by fitting the experimental curves as described previously (40). The phase transitions of three independent experiments were determined and the respective transition midpoints were calculated by differentiation of the increasing part of the curves. We previously showed that the denaturation of MBP did not interfere with the unfolding curves of the PAH protein for ANS fluorescence (4). Protein aggregation based on hydrophobic self-association was determined by RALS. The intensity of scattered light at 335 nm was detected in the right angle to the excitation light of 330 nm upon thermal denaturation of MBP–PAH (0.8 μM PAH subunit). Data points were analyzed by the Boltzman sigmoidal equation for the transition temperatures and the first-order straight-line exponential equation for the slope.

Coupled *in vitro* transcription–translation of PAH

In vitro transcription and translation (TnT) of mouse PAH was carried out using the pcDNA3.1 constructs and the TnT-T7 reticulocyte lysate system (Promega). The TnT reaction was performed for 90 min in the absence or presence of 500 μM BH_4 and 1 mM L-Phe in 2 mM DTT. After stopping the reaction by DNase A and RNase A, the lysates were further incubated at 37°C and aliquots were taken at indicated time points. For PAH activity assays, free amino acids were removed by microcon centrifugal filters (Millipore).

Transient expression of PAH in COS-7

COS-7 cells were maintained in basic RPMI 1640 medium (96 μM L-phenylalanine) with stable glutamine supplemented with 10% fetal bovine serum and 1% antibiotics (PAA). For transient expression of wild-type and V106A-PAH, the pEF-DEST51 cDNA constructs were used. After transfection with 3 μg DNA per 1 million cells using the Amaxa electroporation system (Lonza), cells were cultured for 72 h under three different conditions: (i) basic medium (as described above), (ii) basic medium supplemented with 43 μM BH_4 and 5 μg/ml ascorbic acid (Fluka), (iii) basic medium with 43 μM BH_4, 5 μg/ml ascorbic acid and 1 mM L-Phe. Culture medium was changed every 24 h. Cells were harvested by scraping and lysed by three freeze–thaw cycles in a lysis buffer (SEC buffer containing 1% Triton X-100 and proteinase inhibitors), followed by 20 min centrifugation at 14 000 rpm at 4°C. Both recovered supernatants and pellets resuspended

in lysis buffer were kept at −80°C until being used for SDS–PAGE/immunoblotting and activity assays.

In vivo animal studies

Wild-type (BTBR $T^{+}tf$/J), Pah^{enu1} (BTBR.Cg-Pah^{enu1}/J) and Pah^{enu2} (BTBR-Pah^{enu2}/J) mice were purchased from The Jackson Laboratory and kept under standard conditions. Mouse studies were approved by the Austrian Animal Care and Use Committee in accordance with national and international laws and standards for animal protection. Animals were housed in a controlled temperature room maintained under alternating 12 h light and dark cycles and, in between experiments, had free access to food and water. While Pah^{enu1} and wild-type mice were fed with standard breeder mouse chow (UIZ, Knittelfeld, Austria), Pah^{enu2} mice were kept euphenylalaninemic with a diet devoid of phenylalanine (Teklad 97152) and water containing 30 mg L-phenylalanine. They were placed on standard chow 3 days before the experiments to produce a hyperphenylalaninemic state. The effect of BH_4 (20 μg/g bw b.i.d. by intraperitoneal injection for 3 days) or placebo (NaCl 0.9%, ascorbic acid 0.2%) was assessed on blood phenylalanine concentrations and on *in vivo* phenylalanine oxidation. For this purpose, breath tests were performed in conscious mice. After the i.p. application of ^{13}C-labeled L-phenylalanine (15 μg/g bw, Eurisotop), the mice were placed in individual 100 ml breath chambers with a continuous flow of CO_2-free air for 105 min and breath samples were collected in 6.5 min intervals. For each of the samples, the airflow was discontinued to allow CO_2 levels to accumulate above the limit of quantification (0.8%). At the end of accumulation, the sample was insufflated into an infrared spectrometer (IRIS Wagner Analysen Technik, Germany) for online isotope analysis. The cumulative recovery of ^{13}C in breath samples was calculated based on the $^{13}CO_2/^{12}CO_2$ ratio assuming a total CO_2 production rate of 94 ml/min per g bw × m^2 body surface area. The amount of labeled CO_2 formed was expressed as the cumulative percentage of the dose administered as a function of time. Blood samples for the determination of blood phenylalanine concentrations were collected immediately before the breath test and spotted to filter cards. Then, 3.2 mm spots of these samples were extracted with 200 μl of methanol (containing internal standard) and analyzed by electrospray ionization tandem mass spectrometry. For assessment of PAH activity and PAH protein amount, mice were sacrificed by cervical dislocation 1 h after the last dosage. Liver samples were collected and processed immediately. The liver tissue was homogenized and lysed in a buffer containing 200 mM KCl, 30 mM Tris–HCl, pH 7.25, and proteinase inhibitors. Samples were then centrifuged for 50 min at 4°C and 14 000 rpm and resulting supernatants were frozen in liquid nitrogen until being used for SDS–PAGE/immunoblotting and activity assays. Protein concentration was determined using the Bradford assay.

Statistical analyses

Group mean values were compared by Student's unpaired two-tailed *t* test, and one-way analysis of variance with Dunnett's *post hoc* test was applied for multiple comparisons. Statistical analyses were performed using GraphPad Prism 4.0c (GraphPad Software).

SUPPLEMENTARY MATERIAL

Supplementary Material is available at *HMG* online.

ACKNOWLEDGEMENTS

We wish to thank Anja Schultze, Heike Preisler, Bernadette Schmidt, Maria Trieb and Susanne Wullinger for excellent technical assistance and Georg Wietzorrek for assistance with animal husbandry and animal experiments. This article is part of an M.D. thesis to be submitted by A.E. at Ludwig-Maximilians-University, Munich, Germany.

Conflict of Interest statement. None declared.

FUNDING

This work was supported by the Bavarian Genome Research Network (BayGene) and by the Dr Legerlotz-Stiftung Liechtenstein.

REFERENCES

1. Selkoe, D.J. (2004) Cell biology of protein misfolding: the examples of Alzheimer's and Parkinson's diseases. *Nat. Cell Biol.*, **6**, 1054–1061.
2. Soto, C. (2003) Unfolding the role of protein misfolding in neurodegenerative diseases. *Nat. Rev. Neurosci.*, **4**, 49–60.
3. Winklhofer, K.F., Tatzelt, J. and Haass, C. (2008) The two faces of protein misfolding: gain- and loss-of-function in neurodegenerative diseases. *EMBO J.*, **27**, 336–349.
4. Gersting, S.W., Kemter, K.F., Staudigl, M., Messing, D.D., Danecka, M.K., Lagler, F.B., Sommerhoff, C.P., Roscher, A.A. and Muntau, A.C. (2008) Loss of function in phenylketonuria is caused by impaired molecular motions and conformational instability. *Am. J. Hum. Genet.*, **83**, 5–17.
5. Conn, P.M., Ulloa-Aguirre, A., Ito, J. and Janovick, J.A. (2007) G protein-coupled receptor trafficking in health and disease: lessons learned to prepare for therapeutic mutant rescue *in vivo*. *Pharmacol. Rev.*, **59**, 225–250.
6. Balch, W.E., Morimoto, R.I., Dillin, A. and Kelly, J.W. (2008) Adapting proteostasis for disease intervention. *Science*, **319**, 916–919.
7. Mu, T.W., Ong, D.S., Wang, Y.J., Balch, W.E., Yates, J.R. 3rd, Segatori, L. and Kelly, J.W. (2008) Chemical and biological approaches synergize to ameliorate protein-folding diseases. *Cell*, **134**, 769–781.
8. Gregersen, N., Bross, P., Vang, S. and Christensen, J.H. (2006) Protein misfolding and human disease. *Annu. Rev. Genomics Hum. Genet.*, **7**, 103–124.
9. Cohen, F.E. and Kelly, J.W. (2003) Therapeutic approaches to protein-misfolding diseases. *Nature*, **426**, 905–909.
10. Conn, P.M. and Janovick, J.A. (2009) Drug development and the cellular quality control system. *Trends Pharmacol. Sci.*, **30**, 228–233.
11. Powers, E.T., Morimoto, R.I., Dillin, A., Kelly, J.W. and Balch, W.E. (2009) Biological and chemical approaches to diseases of proteostasis deficiency. *Annu. Rev. Biochem.*, **78**, 959–991.
12. Muntau, A.C., Röschinger, W., Habich, M., Demmelmair, H., Hoffmann, B., Sommerhoff, C.P. and Roscher, A.A. (2002) Tetrahydrobiopterin as an alternative treatment for mild phenylketonuria. *N. Engl. J. Med.*, **347**, 2122–2132.
13. Aguado, C., Perez, B., Ugarte, M. and Desviat, L.R. (2006) Analysis of the effect of tetrahydrobiopterin on PAH gene expression in hepatoma cells. *FEBS Lett.*, **580**, 1697–1701.
14. Erlandsen, H., Pey, A.L., Gamez, A., Perez, B., Desviat, L.R., Aguado, C., Koch, R., Surendran, S., Tyring, S., Matalon, R. *et al.* (2004) Correction

of kinetic and stability defects by tetrahydrobiopterin in phenylketonuria patients with certain phenylalanine hydroxylase mutations. *Proc. Natl Acad. Sci. USA*, **101**, 16903–16908.
15. Perez, B., Desviat, L.R., Gomez-Puertas, P., Martinez, A., Stevens, R.C. and Ugarte, M. (2005) Kinetic and stability analysis of PKU mutations identified in BH_4-responsive patients. *Mol. Genet. Metab.*, **86** (Suppl. 1), S11–S16.
16. Pey, A.L., Perez, B., Desviat, L.R., Martinez, M.A., Aguado, C., Erlandsen, H., Gamez, A., Stevens, R.C., Thorolfsson, M., Ugarte, M. *et al.* (2004) Mechanisms underlying responsiveness to tetrahydrobiopterin in mild phenylketonuria mutations. *Hum. Mutat.*, **24**, 388–399.
17. Kure, S., Sato, K., Fujii, K., Aoki, Y., Suzuki, Y., Kato, S. and Matsubara, Y. (2004) Wild-type phenylalanine hydroxylase activity is enhanced by tetrahydrobiopterin supplementation *in vivo*: an implication for therapeutic basis of tetrahydrobiopterin-responsive phenylalanine hydroxylase deficiency. *Mol. Genet. Metab.*, **83**, 150–156.
18. Scavelli, R., Ding, Z., Blau, N., Haavik, J., Martinez, A. and Thony, B. (2005) Stimulation of hepatic phenylalanine hydroxylase activity but not Pah-mRNA expression upon oral loading of tetrahydrobiopterin in normal mice. *Mol. Genet. Metab.*, **86** (Suppl. 1), S153–S155.
19. Thöny, B., Ding, Z. and Martinez, A. (2004) Tetrahydrobiopterin protects phenylalanine hydroxylase activity *in vivo*: implications for tetrahydrobiopterin-responsive hyperphenylalaninemia. *FEBS Lett.*, **577**, 507–511.
20. McDonald, J.D. and Charlton, C.K. (1997) Characterization of mutations at the mouse phenylalanine hydroxylase locus. *Genomics*, **39**, 402–405.
21. McDonald, J.D., Bode, V.C., Dove, W.F. and Shedlovsky, A. (1990) Pahhph-5: a mouse mutant deficient in phenylalanine hydroxylase. *Proc. Natl Acad. Sci. USA*, **87**, 1965–1967.
22. Sarkissian, C.N., Boulais, D.M., McDonald, J.D. and Scriver, C.R. (2000) A heteroallelic mutant mouse model: a new orthologue for human hyperphenylalaninemia. *Mol. Genet. Metab.*, **69**, 188–194.
23. Shedlovsky, A., McDonald, J.D., Symula, D. and Dove, W.F. (1993) Mouse models of human phenylketonuria. *Genetics*, **134**, 1205–1210.
24. McDonald, J.D., Andriolo, M., Cali, F., Mirisola, M., Puglisi-Allegra, S., Romano, V., Sarkissian, C.N. and Smith, C.B. (2002) The phenylketonuria mouse model: a meeting review. *Mol. Genet. Metab.*, **76**, 256–261.
25. Ledley, F.D., Grenett, H.E., Dunbar, B.S. and Woo, S.L. (1990) Mouse phenylalanine hydroxylase. Homology and divergence from human phenylalanine hydroxylase. *Biochem. J.*, **267**, 399–405.
26. Treacy, E.P., Delente, J.J., Elkas, G., Carter, K., Lambert, M., Waters, P.J. and Scriver, C.R. (1997) Analysis of phenylalanine hydroxylase genotypes and hyperphenylalaninemia phenotypes using L-[1-13C]phenylalanine oxidation rates *in vivo*: a pilot study. *Pediatr. Res.*, **42**, 430–435.
27. Martinez, A., Knappskog, P.M., Olafsdottir, S., Doskeland, A.P., Eiken, H.G., Svebak, R.M., Bozzini, M., Apold, J. and Flatmark, T. (1995) Expression of recombinant human phenylalanine hydroxylase as fusion protein in *Escherichia coli* circumvents proteolytic degradation by host cell proteases. Isolation and characterization of the wild-type enzyme. *Biochem. J.*, **306** (Pt 2), 589–597.
28. Kappock, T.J., Harkins, P.C., Friedenberg, S. and Caradonna, J.P. (1995) Spectroscopic and kinetic properties of unphosphorylated rat hepatic phenylalanine hydroxylase expressed in *Escherichia coli*. Comparison of resting and activated states. *J. Biol. Chem.*, **270**, 30532–30544.
29. Thorolfsson, M., Ibarra-Molero, B., Fojan, P., Petersen, S.B., Sanchez-Ruiz, J.M. and Martinez, A. (2002) L-phenylalanine binding and domain organization in human phenylalanine hydroxylase: a differential scanning calorimetry study. *Biochemistry (Mosc.)*, **41**, 7573–7585.
30. Maier, E.M., Gersting, S.W., Kemter, K.F., Jank, J.M., Reindl, M., Messing, D.D., Truger, M.S., Sommerhoff, C.P. and Muntau, A.C. (2009) Protein misfolding is the molecular mechanism underlying MCADD identified in newborn screening. *Hum. Mol. Genet.*, **18**, 1612–1623.
31. Fontana, A., de Laureto, P.P., Spolaore, B., Frare, E., Picotti, P. and Zambonin, M. (2004) Probing protein structure by limited proteolysis. *Acta Biochim. Pol.*, **51**, 299–321.
32. Mitnaul, L.J. and Shiman, R. (1995) Coordinate regulation of tetrahydrobiopterin turnover and phenylalanine hydroxylase activity in rat liver cells. *Proc. Natl Acad. Sci. USA*, **92**, 885–889.
33. Xia, T., Gray, D.W. and Shiman, R. (1994) Regulation of rat liver phenylalanine hydroxylase. III. Control of catalysis by (6R)-tetrahydrobiopterin and phenylalanine. *J. Biol. Chem.*, **269**, 24657–24665.
34. Shiman, R. and Gray, D.W. (1980) Substrate activation of phenylalanine hydroxylase. A kinetic characterization. *J. Biol. Chem.*, **255**, 4793–4800.
35. Stokka, A.J., Carvalho, R.N., Barroso, J.F. and Flatmark, T. (2004) Probing the role of crystallographically defined/predicted hinge-bending regions in the substrate-induced global conformational transition and catalytic activation of human phenylalanine hydroxylase by single-site mutagenesis. *J. Biol. Chem.*, **279**, 26571–26580.
36. Stokka, A.J. and Flatmark, T. (2003) Substrate-induced conformational transition in human phenylalanine hydroxylase as studied by surface plasmon resonance analyses: the effect of terminal deletions, substrate analogues and phosphorylation. *Biochem. J.*, **369**, 509–518.
37. Andersen, O.A., Flatmark, T. and Hough, E. (2001) High resolution crystal structures of the catalytic domain of human phenylalanine hydroxylase in its catalytically active Fe(II) form and binary complex with tetrahydrobiopterin. *J. Mol. Biol.*, **314**, 279–291.
38. Teigen, K. and Martinez, A. (2003) Probing cofactor specificity in phenylalanine hydroxylase by molecular dynamics simulations. *J. Biomol. Struct. Dyn.*, **20**, 733–740.
39. Kaufman, S. (1993) The phenylalanine hydroxylating system. *Adv. Enzymol. Relat. Areas Mol. Biol.*, **67**, 77–264.
40. Pey, A.L., Ying, M., Cremades, N., Velazquez-Campoy, A., Scherer, T., Thöny, B., Sancho, J. and Martinez, A. (2008) Identification of pharmacological chaperones as potential therapeutic agents to treat phenylketonuria. *J. Clin. Invest.*, **118**, 2858–2867.
41. Miranda, F.F., Teigen, K., Thorolfsson, M., Svebak, R.M., Knappskog, P.M., Flatmark, T. and Martinez, A. (2002) Phosphorylation and mutations of Ser(16) in human phenylalanine hydroxylase. Kinetic and structural effects. *J. Biol. Chem.*, **277**, 40937–40943.